A Multivariate Approach to Estimate Complexity of FMRI Time Series

Henry Schütze[1,2], Thomas Martinetz[1],
Silke Anders[2], and Amir Madany Mamlouk[1]

[1] Institute for Neuro- and Bioinformatics,
[2] Department of Neurology and Neuroimage Nord
University of Lübeck
Ratzeburger Allee 160, 23562 Lübeck, Germany
schuetze@inb.uni-luebeck.de

Abstract. Modern functional brain imaging methods (e.g. functional magnetic resonance imaging, fMRI) produce large amounts of data. To adequately describe the underlying neural processes, data analysis methods are required that are capable to map changes of high-dimensional spatio-temporal patterns over time. In this paper, we introduce Multivariate Principal Subspace Entropy (MPSE), a multivariate entropy approach that estimates spatio-temporal complexity of fMRI time series. In a temporally sliding window, MPSE measures the differential entropy of an assumed multivariate Gaussian density, with parameters that are estimated based on low-dimensional principal subspace projections of fMRI images. First, we apply MPSE to simulated time series to test how reliably it can differentiate between state phases that differ only in their intrinsic dimensionality. Secondly, we apply MPSE to real-world fMRI data of subjects who were scanned during an emotional task. Our findings suggest that MPSE might be a valid descriptor of spatio-temporal complexity of brain states.

Keywords: spatio-temporal complexity estimation, multivariate entropy, fMRI data.

1 Introduction

Traditionally, data analysis in fMRI (functional magnetic resonance imaging) has heavily relied on mass univaritate approaches that consider the time course of each volume element (voxel) in isolation [4]. However, these methods may fail to detect neural processes that lead to significant changes in widely distributed and heavily interconnected neural networks, but are too subtle to cause detectable changes in the local signal. Hence, multivariate approaches seem indispensable in thorough fMRI data analysis.

Dhamala et al. (2002) used the *correlation dimension* to estimate spatio-temporal complexity of brain activity in a task-driven fMRI study. The authors

A.E.P. Villa et al. (Eds.): ICANN 2012, Part II, LNCS 7553, pp. 540–547, 2012.

showed that their measure of complexity was directly related to task difficulty and mental load during task performance [3]. However, the measure proposed by Dhamala et al. (2002) requires large sample sizes and depends on manual inspection steps, two requirements that constrain the usefulness of this measure for the analysis of fMRI data.

Here, we propose a new method to estimate spatio-temporal complexity of brain states that is based on multivariate entropy. Unlike in [3], our aim is to describe changes of global brain states over time rather than globally describe complexity. One common assumption is that complexity is strongly related to information content. Hence, entropy functions, which are by definition information measures [7], are well-suited candidates to estimate complexity. An intuitive approach to estimate complexity of brain states would be to compute the multivariate differential entropy with respect to the corresponding functional images. Unfortunately, we do not know the probability density function (pdf) that is necessary for this estimation. If we assume that the functional images are Gaussian distributed multivariate samples, the differential entropy can be computed by evaluating a closed-form expression. However, estimating the required Gaussian distribution parameters from high-dimensional, low sample size data prohibits a straightforward entropy computation.

In the following, we will introduce Multivariate Principal Subspace Entropy (MPSE) and show how it is derived from the differential entropy of multivariate Gaussian distributed data. Then, we apply MPSE to a data set simulated with a simple model to illustrate the main characteristics of MPSE. Subsequently, we present results that were obtained by applying MPSE to task-driven fMRI time series. Finally, we aim to explain our empirical findings by our simple model.

2 Methods

Let $\boldsymbol{X} = [\boldsymbol{x}_1, ..., \boldsymbol{x}_n] \in \mathbb{R}^{d \times n}$ denote a data matrix representing an fMRI time series. Each column $\boldsymbol{x}_t$ of $\boldsymbol{X}$ represents an fMRI image corresponding to a discrete time index $t \in \{1, ..., n\}$. In order to obtain spatio-temporal complexity estimates at individual time indices, a temporally sliding window of an odd size $w \in \mathbb{N}^+$ is employed so that $1 < w < n$. Let $\boldsymbol{X}_\tau = \left[\boldsymbol{x}_{\tau - \lfloor \frac{w}{2} \rfloor}, ..., \boldsymbol{x}_{\tau + \lfloor \frac{w}{2} \rfloor}\right] \in \mathbb{R}^{d \times w}$ denote the data matrix that columnwise contains w windowed images corresponding to a fix central window position $\tau \in \mathcal{T}_w = \{\lceil \frac{w}{2} \rceil, ..., n - \lfloor \frac{w}{2} \rfloor\}$. The corresponding sample covariance matrix $\hat{\boldsymbol{C}}_{\boldsymbol{X}_\tau}$ is defined as

$$\hat{\boldsymbol{C}}_{\boldsymbol{X}_\tau} = \frac{1}{w-1} \sum_{i=\tau-\lfloor \frac{w}{2} \rfloor}^{\tau+\lfloor \frac{w}{2} \rfloor} \left(\boldsymbol{x}_i - \hat{\boldsymbol{\mu}}_{\boldsymbol{X}_\tau}\right)\left(\boldsymbol{x}_i - \hat{\boldsymbol{\mu}}_{\boldsymbol{X}_\tau}\right)^T \quad , \tag{1}$$

where the sample mean $\hat{\boldsymbol{\mu}}_{\boldsymbol{X}_\tau}$ is defined as

$$\hat{\boldsymbol{\mu}}_{\boldsymbol{X}_\tau} = \frac{1}{w} \sum_{i=\tau-\lfloor \frac{w}{2} \rfloor}^{\tau+\lfloor \frac{w}{2} \rfloor} \boldsymbol{x}_i \quad . \tag{2}$$

Since an fMRI time series usually comprises much fewer images (samples) than voxels (dimensions), a sample covariance matrix $\hat{\boldsymbol{C}}_{\boldsymbol{X}_\tau}$ is necessarily rank deficient, i.e. $\mathrm{rk}(\hat{\boldsymbol{C}}_{\boldsymbol{X}_\tau}) \leq w - 1 < d$. Hence, the eigenvalue spectrum $\Lambda(\hat{\boldsymbol{C}}_{\boldsymbol{X}_\tau}) = (\lambda_1, ..., \lambda_d)$ contains at least $d - (w - 1)$ zero eigenvalues.

The aim of the current paper is to estimate the spatio-temporal complexity of a given data matrix $\boldsymbol{X}_\tau$ by employing multivariate differential entropy. It is assumed that the samples $\boldsymbol{X}_\tau$ are observations drawn from a continuous random vector $\boldsymbol{x} \in \mathbb{R}^d$ that has some pdf p. The corresponding differential entropy $\mathrm{H}[p]$ is defined as

$$\mathrm{H}[p] = -\int_{\boldsymbol{x}\in\mathbb{R}^d} p(\boldsymbol{x}) \ln p(\boldsymbol{x}) \, \mathrm{d}\boldsymbol{x} \ .$$

If we assume that p is a Gaussian pdf with a mean vector $\boldsymbol{\mu}$ and a covariance matrix $\boldsymbol{C}$, i.e. $p(\boldsymbol{x})$ is given by $\mathcal{N}(\boldsymbol{x} \mid \boldsymbol{\mu}, \boldsymbol{C})$, then the corresponding differential entropy is given by the closed-form expression (see e.g. [2])

$$\mathrm{H}[p] = \frac{1}{2} \ln |\boldsymbol{C}| + \frac{d}{2}(1 + \ln(2\pi)) \ . \tag{3}$$

Note that (3) essentially depends on the determinant $|\boldsymbol{C}|$ and thereby on the eigenvalue spectrum $\Lambda(\boldsymbol{C})$, since $|\boldsymbol{C}| = \prod_{\lambda_j \in \Lambda(\boldsymbol{C})} \lambda_j$. In order to compute (3) the true Gaussian density parameters $\boldsymbol{\mu}$ and $\boldsymbol{C}$ have to be estimated. This can be done by computing the maximum likelihood estimates of $\boldsymbol{\mu}$ and $\boldsymbol{C}$ based on the data matrix $\boldsymbol{X}_\tau$ that are given by (2) and (1) [2]. As mentioned above, the sample covariance matrix $\hat{\boldsymbol{C}}_{\boldsymbol{X}_\tau}$ is rank deficient. Simply setting $\boldsymbol{C} = \hat{\boldsymbol{C}}_{\boldsymbol{X}_\tau}$ in (3) would lead to a singularity, since $\left|\hat{\boldsymbol{C}}_{\boldsymbol{X}_\tau}\right| = 0$ and $\lim_{x\to 0} \ln x = -\infty$. In order to elude the singularity we evaluate (3) in a lower k-dimensional principal subspace of $\boldsymbol{X}_\tau$ so that $k = \mathrm{rk}(\hat{\boldsymbol{C}}_{\boldsymbol{X}_\tau})$.

Let $\tilde{\boldsymbol{X}}_\tau^k \in \mathbb{R}^{k\times w}$ denote the data matrix containing the k-dimensional principal subspace projections of the mean subtracted samples of $\boldsymbol{X}_\tau$, i.e.

$$\tilde{\boldsymbol{X}}_\tau^k = \boldsymbol{U}^k(\hat{\boldsymbol{C}}_{\boldsymbol{X}_\tau})^T(\boldsymbol{X}_\tau - (\hat{\boldsymbol{\mu}}_{\boldsymbol{X}_\tau}\mathbf{1}_w^T)) \ ,$$

where $\boldsymbol{U}^k(\hat{\boldsymbol{C}}_{\boldsymbol{X}_\tau}) = [\boldsymbol{u}_1, ..., \boldsymbol{u}_k] \in \mathbb{R}^{d\times k}$ denotes the matrix that contains the unit eigenvectors of $\hat{\boldsymbol{C}}_{\boldsymbol{X}_\tau}$ corresponding to its k largest eigenvalues. By construction the sample covariance matrix $\hat{\boldsymbol{C}}_{\tilde{\boldsymbol{X}}_\tau^k}$ is diagonal and contains the k leading eigenvalues of $\hat{\boldsymbol{C}}_{\boldsymbol{X}_\tau}$ as diagonal elements. Note that $\mathrm{diag}(\hat{\boldsymbol{C}}_{\tilde{\boldsymbol{X}}_\tau^k}) \triangleq \Lambda(\hat{\boldsymbol{C}}_{\tilde{\boldsymbol{X}}_\tau^k})$. Since k is choosen so that $k = \mathrm{rk}(\hat{\boldsymbol{C}}_{\boldsymbol{X}_\tau})$, the rank sufficiency of $\hat{\boldsymbol{C}}_{\tilde{\boldsymbol{X}}_\tau^k}$ follows, i.e. $\mathrm{rk}(\hat{\boldsymbol{C}}_{\tilde{\boldsymbol{X}}_\tau^k}) = k$. Let $\tilde{\boldsymbol{x}}^k \in \mathbb{R}^k$ denote the random vector representing the k-dimensional principal subspace projection of $\boldsymbol{x}$ subject to $\boldsymbol{U}^k(\hat{\boldsymbol{C}}_{\boldsymbol{X}_\tau})$. Then the pdf $q(\tilde{\boldsymbol{x}}^k)$ is given by $\mathcal{N}(\tilde{\boldsymbol{x}}^k \mid \mathbf{0}_k, \hat{\boldsymbol{C}}_{\tilde{\boldsymbol{X}}_\tau^k})$ and the corresponding differential entropy is

$$\mathrm{H}[q] = \frac{1}{2} \ln \left|\hat{\boldsymbol{C}}_{\tilde{\boldsymbol{X}}_\tau^k}\right| + \frac{k}{2}(1 + \ln(2\pi)) \ . \tag{4}$$

Note that the differential entropy (4) is well-defined due to the rank sufficiency of $\hat{\boldsymbol{C}}_{\tilde{\boldsymbol{X}}_\tau^k}$. We call this quantity Multivariate Principal Subspace Entropy (MPSE). $\mathrm{MPSE}(\boldsymbol{X}_\tau)$ can be computed as follows:

$$\begin{aligned}\mathrm{MPSE}(\boldsymbol{X}_\tau) = H[q] &= \frac{1}{2}\ln\prod_{j=1}^{k}\lambda_j + \frac{k}{2}(1+\ln(2\pi)) \\ &= \frac{1}{2}\sum_{j=1}^{k}\ln\lambda_j + \frac{k}{2}(1+\ln(2\pi)) \ . \end{aligned} \tag{5}$$

A multivariate Gaussian distribution is a unimodal distribution, i.e. its entropy depends on its generalized variance, which is given by the determinant of the covariance matrix (see e.g. [6]). If the generalized variance in the principal subspace increases (decreases), MPSE given by (5) also increases (decreases). Note that in contrast to the discrete Shannon entropy the differential entropy and thus MPSE is not bounded and not necessarily nonnegative [2].

3 Data

3.1 Simulated Data

To assess the behavior of the spatio-temporal complexity estimator MPSE, we simulated a number of d-variate time series that comprise phases with states of different complexity. To this end, we modeled temporally alternating off-state phases (off-state a) and more complex on-state phases (on-state b). We assume that these two phases are represented by distinct temporally changing processes that lie in orthogonal subspaces of different intrinsic dimensionalities $d_a, d_b \in \mathbb{N}^+$, and also that the on-state phase process is higher dimensional than the off-state phase process, i.e. $d_b > d_a$.

Let $\boldsymbol{X}_a \in \mathbb{R}^{d_a \times n}$ ($\boldsymbol{X}_b \in \mathbb{R}^{d_b \times n}$) be randomly generated by drawing $n \in \mathbb{N}^+$ samples from the d_a-variate (d_b-variate) Gaussian distribution $\mathcal{N}(\boldsymbol{0}_{d_a}, \boldsymbol{I}_{d_a})$ ($\mathcal{N}(\boldsymbol{0}_{d_b}, \boldsymbol{I}_{d_b})$). We furthermore introduce two binary task functions $\boldsymbol{s}_a, \boldsymbol{s}_b \in \{0,1\}^n$ that are used to model the time course of off-state and on-state phases. Finally, a matrix $\boldsymbol{V}$ is used to embed randomly generated low dimensional samples into a much higher d-dimensional target space. Let $\boldsymbol{V} \in \mathbb{R}^{d \times (d_a + d_b)}$ be a randomly generated projection matrix consisting of $(d_a + d_b)$ pairwise orthonormal d-dimensional vectors, i.e. $\boldsymbol{V}^T\boldsymbol{V} = \boldsymbol{I}_{(d_a+d_b)}$. Hence, an entire simulated time series $\boldsymbol{X}$ is generated as

$$\boldsymbol{X} = \boldsymbol{V}\begin{bmatrix}\boldsymbol{X}_a \odot (\boldsymbol{1}_{d_a}\,\boldsymbol{s}_a^T) \\ \boldsymbol{X}_b \odot (\boldsymbol{1}_{d_b}\,\boldsymbol{s}_b^T)\end{bmatrix} \ ,$$

where $\odot$ denotes the element-wise matrix product operator.

We chose a target space dimensionality of $d = 5000$. For each simulated time series we modeled five off-state phases of length $n_a \in \mathbb{N}^+$ and four on-state phases of length $n_b \in \mathbb{N}^+$. Two different differences of dimensionality between state b and state a were chosen: (1) a rather large difference (i.e. $d_a = 20$, $d_b = 60$) and (2) a rather small difference (i.e. $d_a = 55$, $d_b = 60$).

In the first simulation setting (*exclusive setting*), we assume that both states a and b are temporally exclusive, i.e. either off-state a or on-state b is active. For this setting, simulation parameters are chosen as follows: $n_a = 15$, $n_b = 10$ (i.e. $n = 5n_a + 4n_b = 115$). In the second simulation setting (*transition setting*), we additionally model a transition phase c for each alternation of states. A transition phase is modeled as the concurrency of off-state a and on-state b, i.e. there are short phases of length $n_c \in \mathbb{N}^+$ in which both states are simultaneously active. In other words, a transition phase does not enforce the states to be temporal exclusive and incorporates that one process has a certain shut down delay as another process already becomes active. Note that the dimensionality of this transition phase is $d_c = d_a + d_b$. For this setting, we chose $n_a = 13$, $n_b = 8$ and $n_c = 2$ (i.e. $n = 5n_a + 4n_b + 8n_c = 113$).

3.2 FMRI Data

In this section we introduce fMRI data from a task-driven fMRI study that has been published elsewhere [1]. Six female subjects participated in an fMRI experiment that comprised ten runs. Each run comprised four emotional periods (20s) alternating with four resting periods (18s - 24s). During an emotional period subjects were asked to submerge themselves into an emotional situation (joy, anger, disgust, fear, sadness) and to facially express their emotional feelings. A single word cue (e.g. 'joy') on a black screen signaled an emotional period. During resting periods subjects were asked to relax. A neutral fixation cross signaled a resting period. There were two runs for each emotion per subject, i.e. 60 fMRI time series in total (6 subjects $\times$ 2 runs $\times$ 5 emotions). Each fMRI time series comprises 80 whole brain functional images, that were acquired with a TR (repetition time) = 2s.

FMRI time series were preprocessed including slice acquisition time correction, concurrent spatial realignment and correction of image distortions by use of individual static field maps, normalization into standard MNI space and spatial smoothing (10 mm Gaussian kernel) using SPM5 [9]. Only voxels within a standard anatomical gray matter brain mask [8] were considered in our analysis (i.e. 46,556 voxels per image). Furthermore, from each voxelwise fMRI time series the temporal mean was subtracted and the linear trend was removed. A detailed description of the fMRI experiment can be found in [1].

4 Results

4.1 Results on Simulated Data

Fig. 1 shows MPSE time courses of the simulated data described in section 3.1 using a window of size $w = 5$.

For the *exclusive setting* in our simulation and a rather large difference in state dimensionality ($d_a = 20$, $d_b = 60$) the MPSE time course shows distinctly higher values during on-state phases than during off-state phases (Fig. 1 (a)).

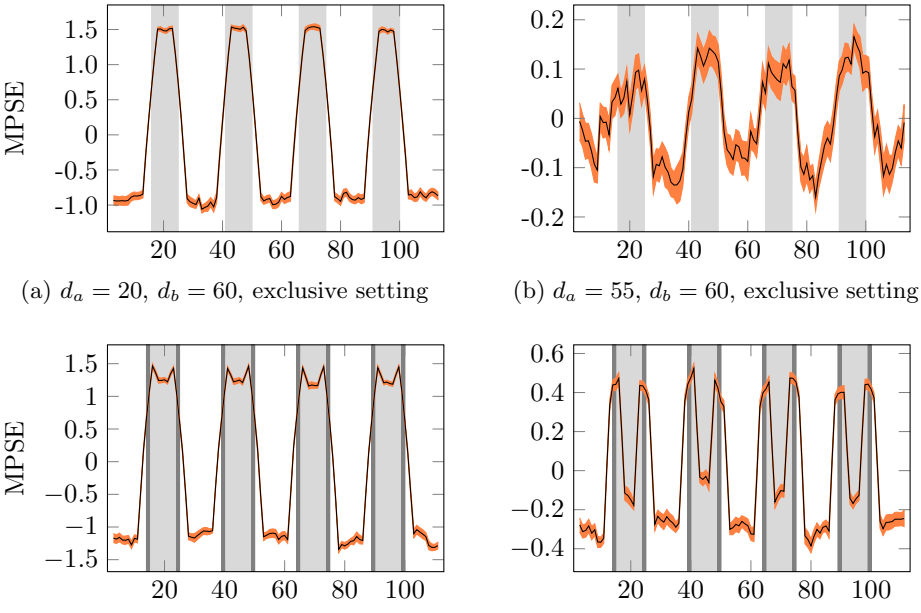

(a) $d_a = 20$, $d_b = 60$, exclusive setting

(b) $d_a = 55$, $d_b = 60$, exclusive setting

(c) $d_a = 20$, $d_b = 60$, transition setting

(d) $d_a = 55$, $d_b = 60$, transition setting

Fig. 1. Average MPSE time courses of simulated time series with standard error (N=30) using a window size $w = 5$. From each single MPSE time course the temporal mean was subtracted before averaging. Light gray (white) bars illustrate simulated on-state (off-state) phases of dimensionality d_b (d_a). Dark gray bars indicate transition phases of dimensionality ($d_a + d_b$).

If in the same simulation setting the difference in state dimensionality is chosen rather small ($d_a = 55$, $d_b = 60$) the MPSE time course still attains high values during on-state phases and low values during off-state phases (Fig. 1 (b)). The on-state to off-state level difference in Fig. 1 (b), however, is smaller compared to Fig. 1 (a). Furthermore, the MPSE time course in Fig. 1 (b) shows stronger high-frequency fluctuations and noise than the MPSE time course in Fig. 1 (a).

For the *transition setting* in our simulation and a rather large difference in state dimensionality ($d_a = 20$, $d_b = 60$) the average MPSE time course shows again a high on-state and a low off-state level. In addition, an even higher third level can be observed during transition phases (Fig. 1 (c)). If in the same simulation setting the difference in state dimensionality is chosen rather small ($d_a = 55$, $d_b = 60$) the transition level can stil be observed (Fig. 1 (d)), but, the MPSE level difference between transition phase and on-state phase increases as the difference in state dimensionality decreases (compare Fig. 1 (c) to Fig. 1 (d)).

4.2 Results on FMRI Data

Fig. 2 shows the average MPSE of the fMRI data set that was described in section 3.2 for windows of size $w \in \{3, 5\}$. Applying MPSE to the fMRI data

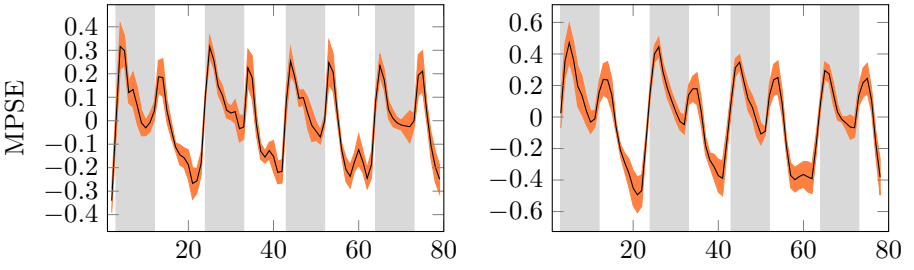

(a) $w = 3$ (b) $w = 5$

Fig. 2. Average MPSE time courses of 60 fMRI time series with standard error across subjects (N=6) using window size w. The temporal mean of each single time course was subtracted before averaging. Gray (white) bars indicate emotional (resting) periods.

obviously results in a time course that reflects the alternation between emotional and resting periods in the fMRI experiment. For both window sizes the average MPSE time course has higher values during emotional periods and lower values during resting periods, i.e. there are task-condition specific levels. Interestingly, the obtained time courses show distinct peaks at task transitions. Increasing the value w from $w = 3$ to $w = 5$ seems to temporally smooth the average MPSE time course. For the larger window $w = 5$ the off-state transition peaks become smaller, but are still clearly visible.

5 Discussion

For simulated data with a large difference in state dimensionality, we showed that MPSE is capable to successfully detect on-state and off-state phases. MPSE considers only w samples at a time and, hence, $(w - 1)$ non-zero eigenvalues due to $w < d_a < d_b$. Although the population eigenvalues are equally sized (isotropic Gaussian model) the estimated eigenvalue spectra give different MPSE levels for different intrinsic dimensionalities (i.e. high MPSE level for high dimensionality and low MPSE level for low dimensionality). This could be explained by the fact that under these high-dimensional, low sample size simulation settings estimated eigenvalues are Marčenko-Pastur distributed [5]. Roughly speaking, as the ratio α between sample size and dimensionality decreases, estimated non-zero eigenvalues and variance of the corresponding spectra increase. Note that the Marčenko-Pastur law actually holds for the asymptotic case of infinite sample sizes for some fix α. Even though we are dealing with very small sample sizes, MPSE increases, due to larger eigenvalue estimates, as the intrinsic dimensionality increases. The same argument explains the high third MPSE level during transition phases. The transition-peaks are rather high compared to the on-state and off-state levels when difference in state dimensionalities is small. This is not surprising, as – by construction – the intrinsic dimensionality of a transition phase is almost twice as high as the dimensionality of an on- or off-state.

For the real-world data, we assumed that during emotional periods brain activity of subjects shows an increased complexity, due to the neural processing induced by the experimental task. During resting periods, in contrast, complexity was expected to decrease. Thus, we expected a correspondence between the time course of a spatio-temporal complexity estimator and the time course of the experimental task. MPSE estimates the time course of the experimental task with high precision. There were significantly higher MPSE levels during emotional than during resting periods. Furthermore, the MPSE time course shows distinct peaks at the state transitions.

In sum, we have introduced MPSE as a measure to estimate spatio-temporal complexity of fMRI time series. We have shown that MPSE is capable to detect different experimental conditions for a real fMRI data set. Entropy levels were higher during emotional periods and lower during resting periods. Furthermore, we found evidence that during transitions between emotional and resting periods complexity increases. Employing a simple model, we could reproduce (1) MPSE level differences and (2) MPSE task transition peaks in simulated time series that comprise state phases of different intrinsic dimensionalities.

Acknowledgement. This work was supported by the DFG, grant number MA 2401/2-1.

References

1. Anders, S., Heinzle, J., Weiskopf, N., Ethofer, T., Haynes, J.D.: Flow of affective information between communicating brains. NeuroImage 54(1), 439–446 (2011)
2. Bishop, C.M.: Pattern Recognition and Machine Learning. Springer, New York (2006)
3. Dhamala, M., Pagnoni, G., Wiesenfeld, K., Berns, G.S.: Measurements of brain activity complexity for varying mental loads. Physical Review E - Statistical, Nonlinear and Soft Matter Physics 65(4), 041917-1–041917-7 (2002)
4. Holmes, A.P., Poline, J.B., Friston, K.J.: Characterizing brain images with the general linear model. In: Human Brain Function, pp. 59–84. Academic Press, USA (1997)
5. Hoyle, D.C.: Automatic PCA Dimension Selection for High Dimensional Data and Small Sample Sizes. Journal of Machine Learning Research 9, 2733–2759 (2008)
6. Johnson, R.A., Wichern, D.W.: Applied Multivariate Statistical Analysis. Prentice Hall, New Jersey (1998)
7. Shannon, C.E.: A Mathematical Theory of Communication. The Bell System Technical Journal 27, 423, 623–656 (1948)
8. Tzourio-Mazoyer, N., Landeau, B., Papathanassiou, D., Crivello, F., Etard, O., Delcroix, N., Mazoyer, B., Joliot, M.: Automated anatomical labeling of activations in spm using a macroscopic anatomical parcellation of the mni mri single-subject brain. NeuroImage 15(1), 273–289 (2002)
9. Wellcome Trust Centre for Neuroimaging, Statistical Parametric Mapping, SPM5, `http://www.fil.ion.ucl.ac.uk/spm/software/spm5/`